

## The coupled dynamics of meltwater percolation and granular deformation in the sediment layer underlying parts of the big ice sheets

A. Damsgaard<sup>1</sup>, A. Cabrales-Vargas<sup>2</sup>, J. Suckale<sup>2</sup>, and L. Goren<sup>3</sup>

<sup>1</sup>Institute of Geophysics and Planetary Physics, Scripps Institution of Oceanography, University of California, San Diego, 9500 Gilman Drive, MC-0225, La Jolla, California 92093-0225, USA; email: [adamsgaard@ucsd.edu](mailto:adamsgaard@ucsd.edu).

<sup>2</sup>Department of Geophysics and Institute of Computational and Mathematical Engineering, Stanford University, Stanford, California, USA.

<sup>3</sup>Ben-Gurion University of the Negev, Geological and Environmental Sciences, Israel.

### ABSTRACT

Ice streams are corridors of fast flowing ice that drain the interiors of the large Antarctic and Greenlandic ice sheets. The abrupt transition from the fast flowing ice of the streams to the almost stagnant ice to their side occurs along narrow shear margins, which experience intense internal deformation. This deformation can lead to warming and weakening of the ice, which makes shear margins prone to migration. Previous studies have suggested that efficient drainage of meltwater at the interface between the ice and the underlying weak sediment layer might control the stability of shear margins. However, weak sediment deformation is expected to be tightly coupled to meltwater drainage, and therefore the feedbacks between them are likely of great importance for ice stream stability, while they remain little understood.

Here, we use a 3D model to capture the dynamic interactions between meltwater percolation and granular deformation. We solve for the granular mechanics using a discrete element algorithm, and compute the flow in the deforming porous media on a superimposed Eulerian grid. The model intends to represent the upper portion of the weak and unconsolidated sediment layer directly beneath the ice in the shear margin. We use it to study (1) how spatial variations in the shearing velocity affect meltwater percolation, and (2) to what degree the till grains are stable in the presence of horizontal gradients in water pressure.

Our simulation results show that horizontal variations in shear velocity enhance the local porosity and permeability, leading to a potentially significant increase in the horizontal water transmissivity. Results further demonstrate that grain stability depends on the magnitude of the horizontal pressure gradient, and cascading events of grain mobilization precede bulk instability flows.

### INTRODUCTION

The Antarctic Ice Sheet exhibits astonishing spatial and temporal variability in ice-flow rate and associated mass loss. Rapid ice flow is concentrated in narrow

corridors called *ice streams* that together with outlet glaciers account for approximately 90% of the current mass loss from the ice-sheet interior to the ocean (e.g. Bamber et al., 2000; Rignot et al., 2011). The response of the ice streams to climatically induced perturbations is hence highly consequential for future projections of sea level (e.g. Scambos et al., 2004; Rignot et al., 2014). Our understanding of the physical processes that control ice-stream dynamics, however, is too incomplete to reliably assess how ice streams will likely respond to changing environmental conditions.

The abrupt change in velocity at the boundary between the ice stream and the neighboring stagnant ice leads to a zone of intense deformation, known as the *shear margin*. Shear margins remain enigmatic features. They may support nearly 100% of the resistance to ice flow (Raymond et al., 2001) in locations where the weak sedimentary bed that ice streams rest upon supports only small stresses (Tulaczyk et al., 2000; Kamb, 2001). Large concentration of shear stress in the margins may lead to ice-stream widening and flow acceleration (Bindschadler and Vornberger, 1998; Suckale et al., 2014; Perol and Rice, 2015). Consequently, the stability of shear margins can have a profound impact on the ice flux to the ocean.

Many, and possibly most, of the unusual characteristics of ice streams are related to the fact that ice is flowing over weak and unconsolidated sediment, commonly referred to as *till* (e.g. Cuffey and Paterson, 2010). Till is unsorted glacial sediment derived from the erosion and reworking of bedrock or sedimentary deposits by moving ice. The subglacial till layer is likely subject to significant but spatially variable meltwater influx, because the shear margins of active ice streams are at the melting point for several tens to hundreds of meters above the bed due to shear heating (Schoof, 2012; Suckale et al., 2014; Perol and Rice, 2015).

The efficiency of drainage of this meltwater in the shear margins could be very consequential for ice-stream dynamics, because the material strength of the till depends sensitively on the interstitial pore-water pressure (Tulaczyk et al., 2000; Kamb, 2001). Spatially-variable pore pressure created by localized drainage pathways would translate to significant spatial variations in till strength that may stabilize or release ice streams (Perol and Rice, 2015; Platt et al., 2016; Elsworth and Suckale, 2016). In the absence of strong topographic controls, the location and width of ice streams may hence be controlled by meltwater drainage at the ice-till interface (Perol and Rice, 2015; Platt et al., 2016; Elsworth and Suckale, 2016).

Grain-fluid interactions in water saturated till may control the layer rheology by inducing time and space variable frictional strength (Goren et al., 2011), altering basal properties in potentially profound ways. A variety of mechanisms have been proposed to modify the frictional resistance of saturated till, including spatial shear localization (Aharonov et al., 2013), which matches in-situ observations of shallow deformation beneath ice streams (Engelhardt and Kamb, 1998; Kamb, 2001) and episodic weakening and strengthening, as observed at some ice-streaming areas (e.g. Bindschadler et al., 2003) that can potentially be enhanced by direct feedbacks between sediment properties and pore pressure (Iverson, 2010; Goren et al., 2011; Damsgaard et al., 2015;

Damsgaard et al., 2016). Gaining insights into these processes could substantially advance our understanding of the spatial and temporal variability in basal stresses and the spontaneous flow instabilities associated with them (e.g. Sayag and Tziperman, 2008).

Here, we investigate the dynamic coupling between meltwater percolation and granular deformation at the scale of individual sediment grains. Our goal is to identify how gradients in shear velocity and horizontal fluid pressure affect the coupled dynamics of grains and interstitial pore fluid in the shear margin of an active ice stream.

### THE COUPLED GRAINS - PORE FLUID MODEL

#### *Till grains*

We model the granular phase using the Lagrangian soft-body discrete element method (Cundall and Strack, 1979; Damsgaard et al., 2013; Damsgaard et al., 2015). The grains are represented as spheres that interact through a scale-invariant contact model with elasticity and friction (e.g. Ergenzinger et al., 2011), where the contact-normal force between a grain pair  $i$  and  $j$  is determined by:

$$\mathbf{f}_n^{i,j} = \frac{E\pi(r_i + r_j)}{2} \delta_n^{i,j} \mathbf{n}^{i,j}, \quad (1)$$

where  $E$  is Young's modulus,  $r$  is grain radius,  $\delta_n$  is grain overlap, and  $\mathbf{n}$  is the contact-normal vector. We define the contact-parallel (tangential) force as:

$$\mathbf{f}_t^{i,j} = -\min \left\{ \frac{E\pi(r_i + r_j)}{2} \|\delta_t^{i,j}\|, \mu \|\mathbf{f}_n^{i,j}\| \right\} \frac{\delta_t^{i,j}}{\|\delta_t^{i,j}\|} \quad (2)$$

where  $\mu$  is the Coulomb-friction coefficient, and  $\delta_t$  is the tangential displacement along the contact interface which is corrected for contact rotation. During slip, the displacement magnitude  $\delta_t$  does not increase as it represents the elastic tangential strain over the contact. We use the sum of forces and torques to determine grain position by explicit integration of Newton's second law of motion:

$$m^i \frac{\partial^2 \mathbf{x}^i}{\partial t^2} = m^i \mathbf{g} + \sum_{j \in N_c} (\mathbf{f}_n^{i,j} + \mathbf{f}_t^{i,j}) + \mathbf{f}_f^i. \quad (3)$$

$\mathbf{x}$  is the grain position,  $m$  is the grain mass, and  $N_c$  is the list of contacts for grain  $i$ . The fluid-interaction force ( $\mathbf{f}_f$ ) includes a buoyancy component and a local pressure gradient induced fluid drag (or seepage) component:  $\mathbf{f}_f^i = -\rho_f V_g \mathbf{g} - V_g \nabla p_f$ . We resolve grain rotation similarly through conservation of angular momentum after finding the sum of torques:

$$I^i \frac{\partial^2 \Omega^i}{\partial t^2} = \sum_{j \in N_c} \left( - \left( r^i + \frac{\delta_n^{i,j}}{2} \right) \mathbf{n}^{i,j} \times \mathbf{f}_t^{i,j} \right) \quad (4)$$

where  $\Omega$  is the angular position and  $I$  is the moment of inertia.

**Meltwater model**

We solve for the fluid pressure on a superimposed Eulerian grid with rectilinear discretization. The fluid motion is coupled to granular deformation through mutual interpolation, where smooth fields of porosity, permeability, and grain velocity are interpolated from the grain scale to the fluid grid, and fluid pressure gradients are interpolated from the fluid grid to individual grains and incorporated into the seepage force. The transient evolution of fluid pressure is dictated by the rate of pressure diffusion and local rate of porosity change ( $\partial\phi/\partial t$ ):

$$\frac{\partial p_f}{\partial t} = \frac{1}{\beta_f \phi \eta_f} (k \nabla^2 p_f + \nabla p_f \cdot \nabla k) - \frac{1}{\beta_f \phi (1 - \phi)} \left( \frac{\partial \phi}{\partial t} + \bar{\mathbf{v}}_g \cdot \nabla \phi \right) \quad (5)$$

where  $\beta_f$  is the adiabatic fluid compressibility,  $\eta_f$  is the dynamic fluid viscosity, and  $\bar{\mathbf{v}}_g$  is the average grain velocity. The permeability  $k$  governs the rate of fluid-pressure diffusion. We estimate local permeability from local porosity through the empirical Kozeny-Carman relation:  $k = k_c \phi^3 / (1 - \phi)^2$ , where  $k_c$  is a permeability prefactor. The coupling between the solid and fluid phases takes place through a bilinear interpolation scheme (Goren et al., 2011).

**Scaling of simulation parameters**

The steady-state rheology of dense granular materials is strain-rate independent as long as the dimensionless inertia parameter,  $I < 10^{-3}$  (GDR-MiDi, 2004):  $I = \dot{\gamma} \bar{d} \sqrt{\frac{\rho}{N}}$ , where  $\dot{\gamma}$  is the shear strain rate,  $d$  is the mean grain diameter,  $\rho$  is the grain material density, and  $N$  is the effective normal stress. Following Damsgaard et al. (2016), it can be shown that ice-flow velocities yield inertia parameter values in the pseudo-static and rate-independent range, except when pore-water pressures exceed the ice overburden stress. However, we do not expect till rheology to influence ice flow in this case, since very small effective stress facilitates ice-bed decoupling without till deformation. Thus, granular rheology and kinematics are expected to be independent in the till layer.

The explicit integration scheme of the soft-body discrete element method requires very small time steps, necessitating scaling of model time against the real subglacial setting. We shear the granular assemblage with a maximum velocity of  $1.114 \times 10^{-2} \text{ m s}^{-1}$ , three to four orders of magnitude faster than subglacial shear in ice streams (e.g. Cuffey and Paterson, 2010), but still in the pseudo-static and rate-independent regime of granular deformation. To maintain the correct ratio of grain to fluid velocity, we scale the fluid dynamic viscosity  $\eta_f$  in Eq. 5 to a value of  $2.08 \times 10^{-7} \text{ Pa s}$ , which allows rapid diffusion of fluid pressure.

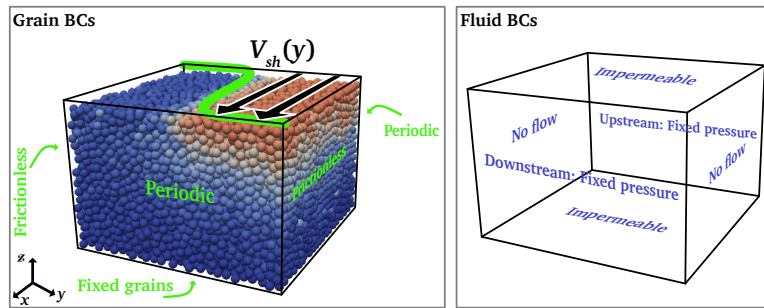


**Figure 1. Boundary conditions for the grain and fluid phases in the applied experimental setup.**

**Setup of the coupled model**

The granular assemblage consists of  $\sim 10,000$  spherical grains in a confined box. The average grain diameter is 0.02 m and grains are close to equi-dimensional, but we prescribe a small size variance to avoid geometrical patterns of regular packing. Despite the wide distribution of grain sizes that has been identified in subglacial tills, we choose to avoid significant polydispersity to increase computational efficiency. Similarly the elastic modulus,  $E$ , used in our model, is smaller by two orders of magnitude with respect to that of quartz grains, which allows us to increase the time step. We do not account for grain crushing which is likely to be negligible for the low effective stresses under ice streams. Initially the grains are placed randomly in space and are allowed to settle at the bottom of the box under the influence of gravity. Then, the assemblage is uniaxially consolidated at a constant confining stress  $N$  until its volumetric strain rate goes to zero, following the procedure in Damsgaard et al. (2013), Damsgaard et al. (2015), and Damsgaard et al. (2016). The boundary conditions for the two phases are visualized in Fig. 1. The source code and simulation scripts are available online (<https://github.com/anders-dc/sphere>).

**RESULTS**

**Flow localization under imposed velocity discontinuities**

The imposed gradient in shear velocity creates a spatial variability in deformation. The fast-moving parts are characterized by a  $\sim 0.2$  m thick shear zone (Fig. 2, left), corresponding to ten grain diameters. The shear zone thickness rapidly decreases as the imposed shear velocity goes to zero. The deformation pattern causes variability in horizontal and vertical shear-strain rates across the simulation domain. Dilation patterns and internal porosity trends are well investigated in simple shear experiments on confined granular assemblages (e.g. Damsgaard et al., 2013; Aharonov et al., 2013). In this experiment we observe that the addition of horizontal, shear transverse, components to the shear strain tensor enhance porosities further (Fig. 2, middle). Hydraulic permeability is non-linearly linked to porosity, which results in large hydraulic conductivity and water flux adjacent to the imposed shear discontinuity (Fig. 2, right). Addition-

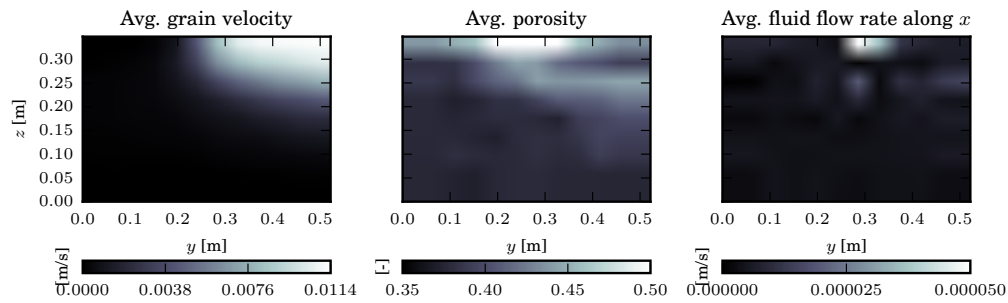


**Figure 2. Critical (steady) state grain and fluid dynamics across the imposed gradient in shear velocity. Spatial differences in particle velocities (left) enhance porosities locally (center), which increases fluid-transport capacity beneath the shear zone (right). The right panel shows fluid velocity relative to grain velocity.**

ally, water flow is slightly enhanced in the porous shear zone beneath the fast-moving section ( $y = 0.3$  to  $0.5$  m in Fig. 2, right panel).

***Granular stability against gradients of horizontal fluid pressure***

The sediment beneath ice-stream shear margins is likely to contain substantial spatial gradients in water pressure due to differential water input into the bed. Seepage forces drag grains opposite of the fluid-pressure gradient. Unlike fluidization, where the fluid forces balance or exceed grain gravitational acceleration, horizontal gradients of fluid-pressure can induce grain movement when the seepage forces exceed frictional resistance. Ignoring the imposed shear stress and grain rotation, we can approximate this relationship as a stability criterion:

$$\mu \|\mathbf{f}_z\| \geq \|\nabla p_{f,xy}\| V_g \tag{6}$$

where  $\mu$  is the grain frictional coefficient,  $\mathbf{f}_z$  is the vertical compressive force on the grain,  $\nabla p_f$  is the gradient in fluid pressure, and  $V_g$  is the grain volume. We expect that some grains are more susceptible to mobilization since they are located between load-bearing force chains, and even small gradients in fluid pressure will mobilize them. Once moving, they can push other grains and can cause a cascade of events. Future investigations will focus on backtracing observed instability events at the grain scale.

We performed several simulations with different values for the fluid-pressure gradient ( $dp_f/dx$ ) in order to explore the stability frontier (Fig. 3). With increasing pressure-gradient values we observe that the imposed shear deformation deepens as the seepage force influences the internal force balance by adding a drag along  $x$  (the shear direction). The simulation with the largest value for the fluid-pressure gradient (Fig. 3, right) shows continued unstable grain movement from  $t = \sim 25$  s and onward as

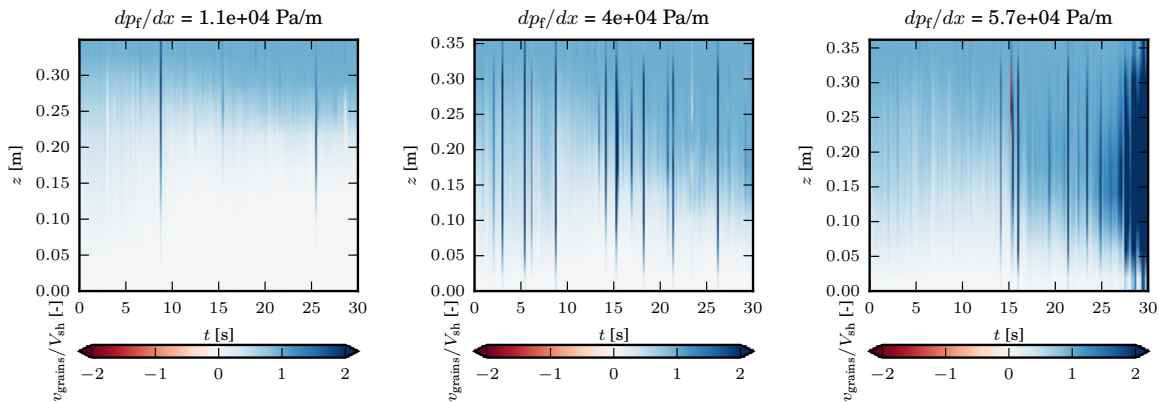


**Figure 3. Grain velocities ( $v_{\text{grains}}$ ) in the moving part ( $y \in [0.3; 0.5]$  m) normalized against the imposed shear velocity ( $V_{\text{sh}}$ ), and plotted with depth (vertical axes) over time (horizontal axes). The three panels represent different simulations with different imposed horizontal gradients in pore-water pressure ( $dp_f/dx$ ). Dark blue colors ( $v_{\text{grains}}/V_{\text{sh}} > 1$ ) correspond to events where the horizontal fluid-pressure gradient is sufficient to mobilize the sediment beyond the imposed shear velocity.**

the granular assemblage approaches its critical and more dilute state. The mobilization is observed to initiate at intermediate depths. These results indicate that the stability of the subglacial till layer is sensitive to gradients in pore-water pressure, but with dynamical thresholds tied to its frictional properties.

**CONCLUSIONS**

Ice streams are of first-order importance to ice-sheet dynamics, but the physical processes determining the positioning of their lateral shear margins are not well understood. We apply the discrete element method coupled with a pore-pressure model in order to understand mechanical, structural, and hydrological patterns associated with the velocity transitions in the subglacial bed across an ice-stream shear margin with meltwater influx. We observe that the velocity transition creates zones of elevated porosity that are more capable of transporting subglacial water. This preferential flow pattern may be important for enhancing the strength of the sediment at the ice base and facilitate stability of the ice-stream shear margin. Furthermore, the enhanced fluid flux may initiate fingering instabilities (e.g. Mahadevan et al., 2012), which may increase hydraulic transmissivity and basal strengthening even further. We investigate sediment stability under horizontal gradients in water pressure in order to understand if flux-driven erosion may initiate channelized drainage under ice-stream shear margins. Sediment stability against mobilization is likely to be governed by a distinct limit dependent on confining pressure, friction, sediment state, and fluid-pressure gradients. We observe that as the fluid-pressure gradient increases, grain layers become unstable and move rapidly downslope with rates that surpass the imposed shear velocity.

## References

- Aharonov, E., L. Goren, D. Sparks, and R. Toussaint (2013). "Localization of Shear in Saturated Granular Media: Insights from a Multi-Scaled Granular-Fluid Model". In: *Fifth Biot Conference on Poromechanics*. Ed. by C. Hellmich, B. Pichler, and D. Adam. Vienna, Austria: American Society of Civil Engineers, pp. 471–480. DOI: 10.1061/9780784412992.049.
- Bamber, J. L., D. G. Vaughan, and I. Joughin (2000). "Widespread complex flow in the interior of the Antarctic ice sheet". In: *Science* 287.5456, pp. 1248–1250.
- Bindschadler, R. A., M. A. King, R. B. Alley, S. Anandakrishnan, and L. Padman (2003). "Tidally controlled stick-slip discharge of a West Antarctic ice". In: *Science* 301.5636, pp. 1087–1089.
- Bindschadler, R. and P. L. Vornberger (1998). "Changes in the West Antarctic Ice Sheet Since 1963 from Declassified Satellite Photography". In: *Science* 279.5351, pp. 689–692. DOI: 10.1126/science.279.5351.689.
- Cuffey, K. M. and W. S. B. Paterson (2010). "The Physics of Glaciers". In: *Elsevier* 4, p. 693.
- Cundall, P. A and O. D. L. Strack (1979). "A discrete numerical model for granular assemblies". In: *Géotechnique* 29, pp. 47–65. DOI: 10.1680/geot.1979.29.1.47.
- Damsgaard, A., D. L. Egholm, J. A. Piotrowski, S. Tulaczyk, N. K. Larsen, and K. Tylmann (2013). "Discrete element modeling of subglacial sediment deformation". In: *J. Geophys. Res. Earth Surf.* 118, pp. 2230–2242. DOI: 10.1002/2013JF002830.
- Damsgaard, A., D. L. Egholm, J. A. Piotrowski, S. Tulaczyk, N. K. Larsen, and C. F. Brødstrup (2015). "A new methodology to simulate subglacial deformation of water-saturated granular material". In: *The Cryosphere* 9, pp. 2183–2200. DOI: 10.5194/tc-9-2183-2015.
- Damsgaard, A., D. L. Egholm, L. H. Beem, S. Tulaczyk, N. K. Larsen, J. A. Piotrowski, and M. R. Siegfried (2016). "Ice-flow dynamics forced by water-pressure variations in subglacial granular beds". In: *Geophysical Research Letters* 43. DOI: 10.1002/2016gl071579.
- Elsworth, C. W. and J. Suckale (2016). "Rapid ice flow rearrangement induced by subglacial drainage in West Antarctica". In: *Geophysical Research Letters* 43.22, pp. 11,697–11,707. DOI: 10.1002/2016gl070430.
- Engelhardt, H. and B. Kamb (1998). "Basal sliding of ice stream B, West Antarctica". In: *J. Glaciol.* 44.147, pp. 223–230.
- Ergenzinger, C., R. Seifried, and P. Eberhard (2011). "A discrete element model to describe failure of strong rock in uniaxial compression". In: *Granul. Matter* 13, pp. 341–364. DOI: 10.1007/s10035-010-0230-7.
- GDR-MiDi (2004). "On dense granular flows". In: *European Physics Journal E* 14, pp. 341–365.

- Goren, L., E. Aharonov, D. Sparks, and R. Toussaint (2011). "The mechanical coupling of fluid-filled granular material under shear". In: *Pure and Applied Geophysics* 168.12, pp. 2289–2323. DOI: 10.1007/s00024-011-0320-4.
- Iverson, N. R. (2010). "Shear resistance and continuity of subglacial till: hydrology rules". In: *J. Glaciol.* 56.200, p. 1104.
- Kamb, B. (2001). "Basal zone of the West Antarctic ice streams and its role in lubrication of their rapid motion". In: *The West Antarctic Ice Sheet: Behavior and Environment*, pp. 157–199.
- Mahadevan, A., A. V. Orpe, A. Kudrolli, and L. Mahadevan (2012). "Flow-induced channelization in a porous medium". In: *Eur. Phys. Lett.* 98.5, p. 58003. DOI: 10.1209/0295-5075/98/58003.
- Perol, T. and J. R. Rice (2015). "Shear heating and weakening of the margins of West Antarctic ice streams". In: *Geophys. Res. Lett.* 42.9, pp. 3406–3413. DOI: 10.1002/2015GL063638.
- Platt, J. D., J. Suckale, T. Perol, and J. R. Rice (2016). "Determining conditions that allow a shear margin to coincide with a Röthlisberger channel". In: *Journal of Geophysical Research* 121, pp. 1–23.
- Raymond, C. F., K. A. Echelmeyer, I. M. Whillans, and C. S. M. Doake (2001). "Ice stream shear margins". In: *The West Antarctic Ice Sheet: Behavior and Environment*. Vol. 77. American Geophysical Union. Chap. Ice Stream, pp. 137–155.
- Rignot, E., J. Mouginot, and B. Scheuchl (2011). "Ice flow of the Antarctic ice sheet". In: *Science* 333.6048, pp. 1427–1430.
- Rignot, E., J. Mouginot, M. Morlighem, H. Seroussi, and B. Scheuchl (2014). "Widespread, rapid grounding line retreat of Pine Island, Thwaites, Smith, and Kohler glaciers, West Antarctica, from 1992 to 2011". In: *Geophysical Research Letters* 41.10, pp. 3502–3509. DOI: 10.1002/2014g1060140.
- Sayag, R. and E. Tziperman (2008). "Spontaneous generation of pure ice streams via flow instability: Role of longitudinal shear stresses and subglacial till". In: *Journal of Geophysical Research* 113.B5.
- Scambos, T. A., J. A. Bohlander, C. A. Shuman, and P. Skvarca (2004). "Glacier acceleration and thinning after ice shelf collapse in the Larsen B embayment, Antarctica". In: *Geophysical Research Letters* 31.18. DOI: 10.1029/2004g1020670.
- Schoof, C. (2012). "Thermally driven migration of ice-stream shear margins". In: *Journal of Fluid Mechanics* 712, pp. 552–578. DOI: 10.1017/jfm.2012.438.
- Suckale, J., J. D. Platt, T. Perol, and J. R. Rice (2014). "Deformation-induced melting in the margins of the West Antarctic ice streams". In: *J. Geophys. Res. Earth Surf.* 119.5, pp. 1004–1025. DOI: 10.1002/2013JF003008.
- Tulaczyk, S., W. B. Kamb, and H. F. Engelhardt (2000). "Basal mechanics of ice stream B, West Antarctica I. Till mechanics". In: *J. Geophys. Res.* 105.B1, pp. 463–481. DOI: 10.1029/1999JB900329.